

CASE-STUDY OF THE RHINE RIVER and LAKE of CONSTANCE

HYDROCOASTAL PROJECT

SUB-CONTRACT [SATOC-CNR] TO RACZIW CONTRACT N. [4000129872/20/I-DT]

Luciana Fenoglio, Hakan Uyanik, Jiming Chen, University Bonn, Germany fenoglio@uni-bonn.de

1. Introduction

The River Rhine originates in the Swiss Alps and flows over a distance of 1,233 km into the North Sea. Its catchment area spans nine countries. Some of the water from the Alps is temporarily stored in alpine reservoirs and flows through large lakes at the edge of the Alps, such as the Lake of Constance and the lakes along the Jura mountains (Fig.1.1).

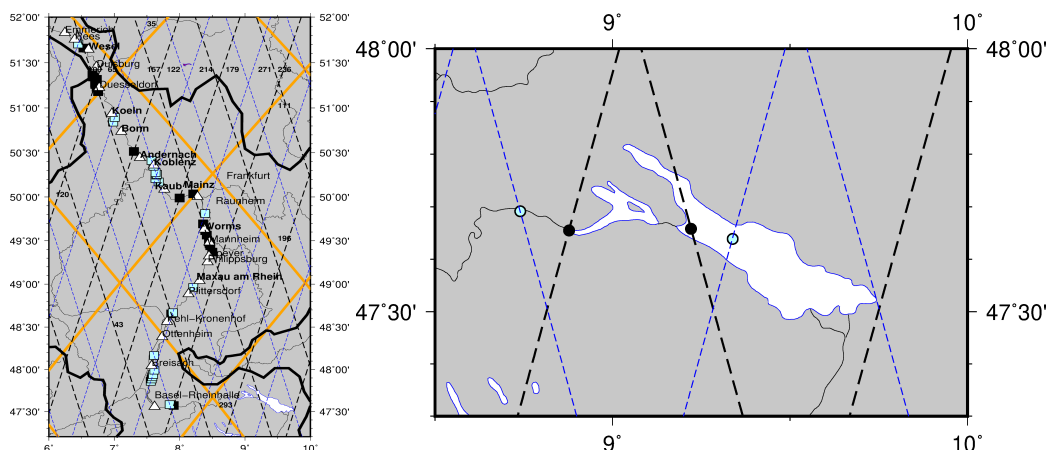


Figure 1.1. Inland Water case study on the River Rhine with Sentinel-3A/3B/6A ground tracks and locations of fiducial reference data from operational tide gauges of the BfG network (left). Lake of Constance (right).

Below Basel, substantial tributaries join from the upland ranges of Germany and France, such as the Neckar, Main, and Moselle, feeding into the Rhine in the Netherlands. Here, the Rhine branches and the Meuse (Maas) form a delta. The Rhine connects important economic regions between the Alps and the North Sea. Around 58 million people live in its basin area. The Rhine's water is used as drinking water, for power generation, for irrigation, for industrial production, and for the transportation of goods. Consequently, it is one of the most intensively-utilized rivers in Europe and one of the busiest waterways in the world. At the same time, it is also an important habitat for wildlife and plants.

The Rhine's streamflow stems from rain and, especially in spring and summer, also from snowmelt and glacier ice melt. As a result of global warming, the Alpine glaciers are melting and winter snowpack is progressively declining. Surface water level, river discharge and water storage change are sensible indicators of long-term change of water cycle within a river catchment. Recently, low water levels in the river Rhine made navigation difficult, while high water levels due to intense rain events caused serious losses. In this study case for inland waters, we compute river discharge from space observations using simple equation including the Manning's roughness coefficient and the parameters water depth, river slope, river width.

The fluvial characteristics of the Rhine river is first investigated using the 17 in-situ stations of the GRDC database (Fig. 1.2). Mean discharge, minimum and maximum over the all interval of availability is computed. The annual cycle, fitted to the data over 10 years slots, shows both a displacement of the maximum of river runoff from May to February and less pronounced seasonality in the last decades.

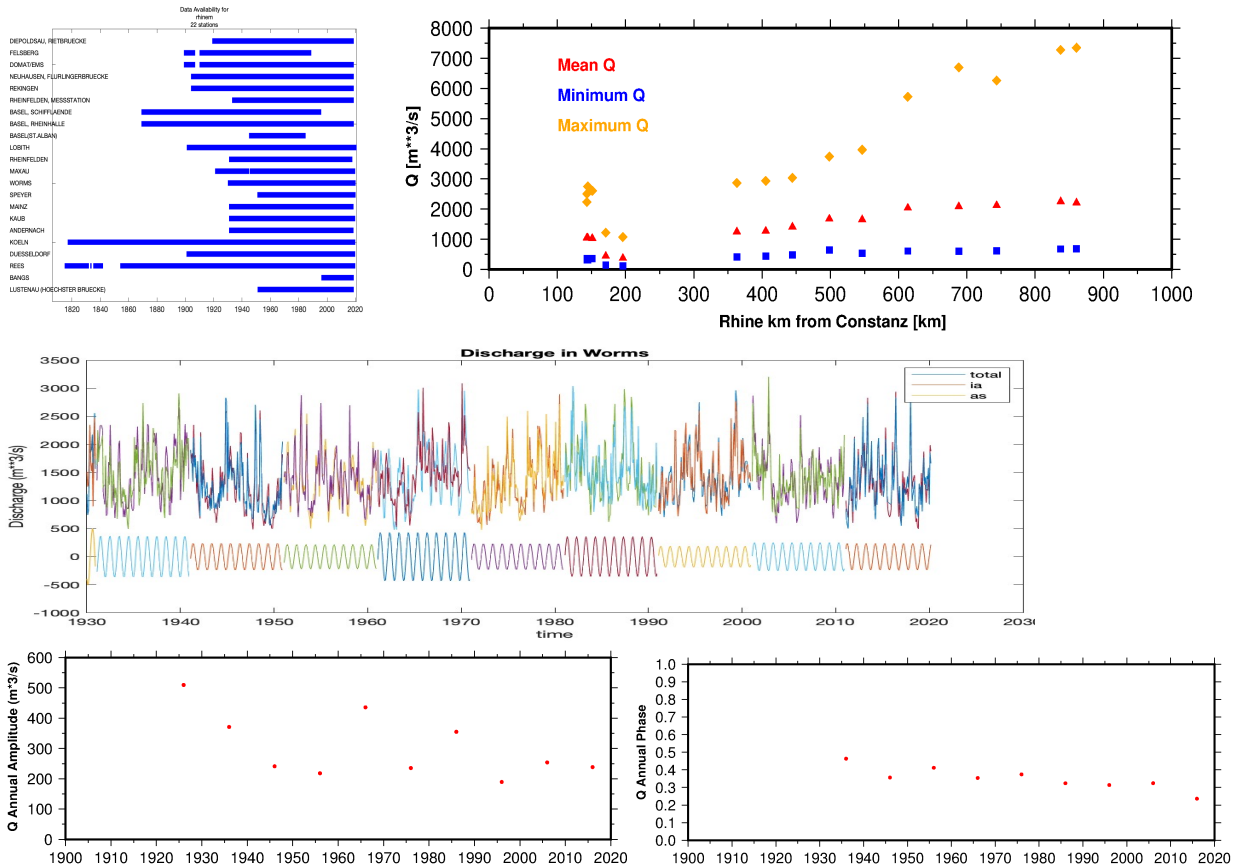


Figure 1.2. GRDC daily discharge data availability until end of 2019 (top left), mean discharge /top right), Discharge in Worms and annual amplitude computed over intervals of 10 years (middle) with time variability in amplitude and phase (bottom).

2. River Rhine and Lakes in Germany

The region is of interest for validation because of the large network of fiducial reference measurements and the hydrodynamic model Sobek available through the German hydrological agencies (BfG). The locations of the Sentinel-3 virtual gauges and of the corresponding in situ high frequency 15 minutes water level measurements are shown in Figure 1.1. Daily discharge are available for a sub-set of the stations from the GRDC database (Fig. 1.2). In this study case the goal is first to evaluate the performance of the altimeter product in terms of accuracy and then to apply the new products to study long-term change and extremes in river runoff and water storage change in glacial lakes and reservoirs .

2.1 Objectives

The main objectives of the impact assessment are:

- to assess the HydroCoastal water level product in German rivers and lakes
- to demonstrate the benefits and the scientific value of an improved inland altimetry product to estimate river runoff and water storage change in lakes and reservoirs.

2.2 Methodology

A land-sea processor for Sentinel-3 was coded in Matlab to assess the performance of the HydroCoastal product. The main functionalities of the processor were: a) read the HydroCoastal product and prepare a mat file with relevant parameters; b) create time series of sea level anomalies, sea surface heights and heights above the geoid for comparison with tide gauges (TG) or for other scientific exploitation; c) inter-compare the HydroCoastal products (DTU, AKH and official ESA products) and to other products selected based on previous analysis. The selected external unfocused SAR product is SAR Versatile Altimetric TOolkit for Research and Exploitation (SARvatore) for Sentinel-3 with the SAMOSA+ retracker, that is available through the EarthConsole

platform (Dinardo et al., 2016). Alternative processing is made with an in-house FFSAR processor with Omega-kappa algorithm and SAMOSA+ retracker.

2.2.1 Quality flags

Values retained for the HydroCoastal data are those with flag set as good. They are:

- flags_dtu Use data with flags [0 and 1] for DTU range
- flags_aks Use data with flags [0 and 1] for AKS range

rain_flag and rad_surf_type were not used. For the ESA range, σ_0 and SWH no flag where considered. Only altimetry measurements collocated on water were considered:

- surf_type Surface Type Flag [0 ocean, 1 enc.seas/lakes, 2 ice, 3 land]

2.2.2 Building water level time-series

As in the validation assessment, all corrections except DAC and ocean tide have been applied to the range.

$$\text{corr_tot} = +\text{dry_tropo} + \text{wet_tropo} + \text{GIM_iono} + \text{solid_earth_tide} + \text{geocentric_polar_tide} + \text{load_tide}$$

Time series are built from satellite altimetry to be compared to the in-situ time series. In rivers, the accuracy of altimetry is evaluated as in the validation part of HYDROCOASTAL using the Virtual pass method. In lakes, instead, the data are binned along track and time series are created at each bin location. While in the virtualpass method we have one time-series per station, in the binning methods several time-series along the ground track are created. The binning strategy is as follows. First the cycle with maximum number of points in the selected track is taken as reference track and all the points are referred from the points in this cycle. Secondly, the corrected data are interpolated according to the reference track. Thirdly, a time series is created at each binned point if corrections and re-tracked range are available, by applying the 3-sigma outlier test.

is applied to evaluate the standard deviation differences (STDD) between gauge and altimetry. Here the data along-track are binned at 20 Hz. The gauge data used in this study are referenced to the zero of the gauge. The height of the zero of the gauge above the German quasi geoid is finally transformed in the ITRF2014 frame to allow a an absolute comparison with the altimeter measurements.

2.2.3 Comparing water level time-series with statistical indicator

We evaluate the standard deviation difference between the altimetric and in-situ time-series. In the virtual pass method one STDD is available per location and we evaluate their mean and median over all the virtual gauges available, as follows:

- mean of STDD
- median of STDD with STDD the standard deviation difference:

$$\bullet \text{ STDD} = \sqrt{\frac{1}{N-1} \sum_{n=1}^N [(X_i - \underline{X}) - (Y_i - \underline{Y})]^2}, \underline{X} = \text{mean}(X)$$

In the binning method we evaluate at each binned time-series the STDD between the altimetric and in-situ time-series. We then select evaluate for each station both options :

- minimum STDD along the track
- median of all STDD along the track

and we compute mean and the median of each of the options over the virtual gauges as above to have an overall statistics.

2.2.4 Computing river runoff from altimeter time-series and auxiliary data

In this study case for inland waters, we compute river discharge from space observations using simple equation including the Manning's roughness coefficient and the parameters water depth, river slope, river width. The key first-order hydraulic parameters, i.e. channel bathymetry and Manning's roughness coefficient are not measurable from space. The depth of the water, that's the water level above the river bottom, is here derived from SAR nadir altimetry over 2016-2023 using a Digital Terrain Model (DTM). The river slope is derived from satellite altimetry as the difference in water

height above the geoid at two virtual gauges located on the same ground track in the same altimeter cycle. The river width is obtained from satellite imagery. The fluvial characteristics of the Rhine river is first investigated. The river width changes less during the year, while changes in heights and slope are more relevant. Mean discharge is computed from 17 in-situ stations of the GRDC database.

Manning coefficient and the exponents of the equation are derived in a least square adjustment at virtual gauges where slope can be computed from altimetry and where 15-min river discharge is available from in-situ nearby stations. The derived discharge is externally validated against in-situ daily GRDC data, against model discharge of the Sobek hydrodynamic model and against discharge from an empirical model GR4J, a catchment water balance model that relates monthly runoff to rainfall and evapotranspiration (<https://webgr.inrae.fr/en/models/daily-hydrological-model-gr4j/description-of-the-gr4j-model/>). The validation is done on a multi-criteria basis, including standard statistical scores such as the correlation coefficient, bias, root mean square error, and Nash-Sutcliffe efficiency.

2.2.4 Computing river runoff from altimeter time-series and auxiliary data

In this study case for inland waters, we compute river discharge from space observations using

2.3 Results

Using the Level 2 Hydrocoastal products, the position of the Virtual Gauges is computed at the intersection between altimeter ground tracks and the river centerline of the hydrodynamic Sobek model. A static mask of the river is used to extract the altimeter data within the river and the Virtualpass method to build the time-series. A total of 42 virtual gauges for Sentinel-3A and Sentinel-3B data are identified with distance smaller than 30 km from the nearest in-situ river gauge. The accuracy of the water level of the DTU product is found to be higher than the accuracy of the original ESA product, that uses the open ocean SAMOSA2 retracker. The highest accuracy in Hydrocoastal products is with the ECMWF wet-tropospheric correction, with median over the 42 VGs equal to 0.355 m. With the UPorto correction the accuracy is very similar (0.37 m). With 80 Hz UFSAR SARvatore processing in Earth Console with the SAMOSA+ retracker the median is 0.27 m. Results are summarized in Table 2.1 below.

The Level 3 DTU Hydrocoastal products consist of DTU time-series at the VG locations, however only 25 of the 42 VGs considered above have a DTU L3 time-series. The median of the STDD with the nearest gauges is 0.40 m and reduces to 0.25 when a sigma-4 criteria is applied. The Level 3 AHL V0.19 Hydrocoastal products consist of DTU time-series at VG locations, in this case 57 VGs are found in this product. The median of the STDD with the nearest gauges is 1.53 m and reduces to 0.26 when a sigma-4 criteria is applied. In Figure 2.2 the sigma-4 criteria is applied.

Table 2.1 River Rhine. Statistics of comparison of altimetric time-series derived from L2 DTU with in-situ data over the 42 VGs

STDD with in-situ (m)	L2toL3 20Hz-DTU ECMWF	L2toL3 20Hz-ESA ECMWF	L2toL3 20Hz-DTU UPorto	L2toL3 20Hz-ESA Uporto	80 Hz SaR/ SAMOSA+
Median	0.355	0.425	0.371	0.424	0.267
Mean	0.807	0.583	0.815	0.583	0.479

Table 2.2 River Rhine. Statistics of comparison of altimetric DTU L3 time-series with in-situ data over a subset of 25 VGs

STDD with in-situ (m)	L3DTU 20Hz-DTU No criteria	L3DTU 20Hz-DTU Sig 4	L3AHL 20Hz-DTU No criteria	L3AHL 20Hz-DTU Sigma 4
Median	0.40	0.25	1.53	0.26
Mean	0.60	0.47	2.15	0.78
Num VG	25	25	57	57

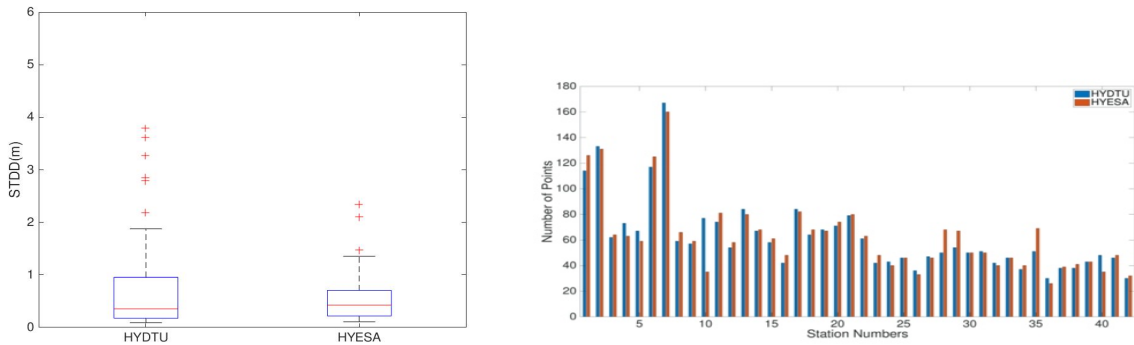


Figure 2.1 Median of STDD with ECMWF wet-tropo correction (left) and corresponding number of observations at the 42 VGs (Fig. 1.1).

Table 3 compares at the VG near Mainz the DTU and AHL L3 results. When the sigma-4 criteria is applied the STDD is around 10 cm. The UFSAR DTU and the ESA 20 Hz time-series are shown together with the dedicated UFSAR Sarvatore SAMOSA+ and the FFSAR SAMP at 20 Hz and 80 Hz in Fig. 2.4. The best accuracy is obtained from FFSAR at 80 Hz (0.155 m). Higher frequencies are preferable along a river. The radargrams in Fig. 2.7 show that FFSAR and higher frequencies are better. The along track data are binned to compute STDD along track.

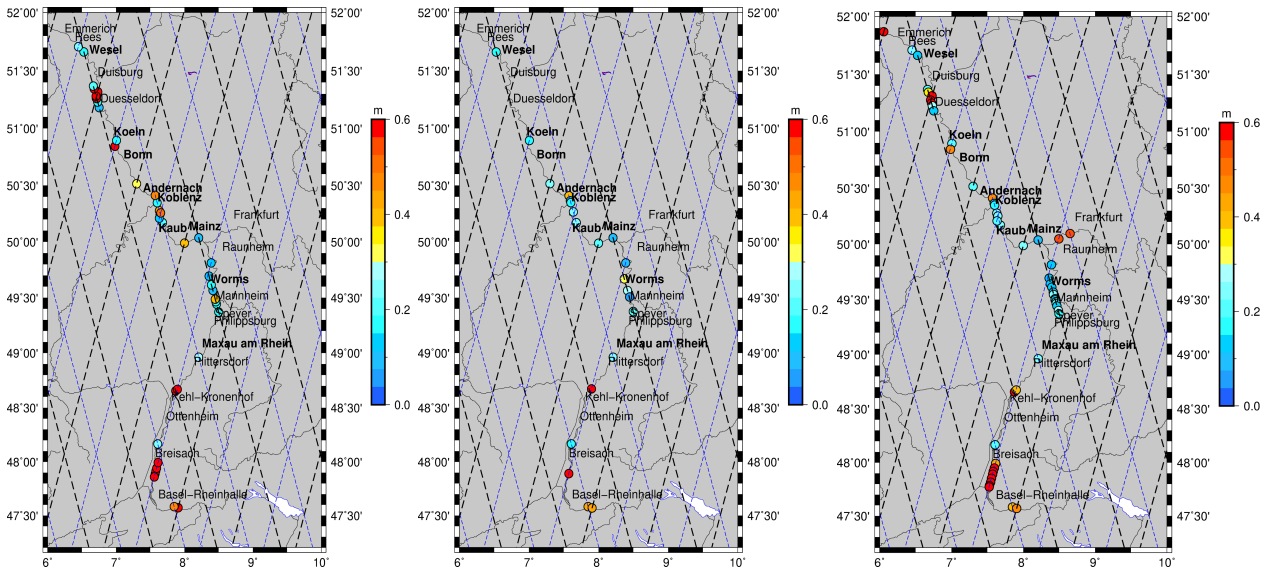


Figure 2.2 STDD between L3 time-series and in-situ for L3-inhouse DTU time-series (42 VG), L3-DTU time-series (25 VGs) and L3-DTU-AHL time-series (57 VG)

Table 2.3 River Rhine. Statistics for Mainz of STDD of altimetric time-series L3 DTU and L3 DTU-AHL with in-situ data

	20Hz-L3 DTU No sigma4	20Hz-L3 DTU Sigma4	20Hz-L3 DTU-AHL No Sigma4	20Hz-L3 DTU- AHL Sigma4
STDD (m)	0.12	0.09	0.16	0.11
Npoints	88	86	85	81

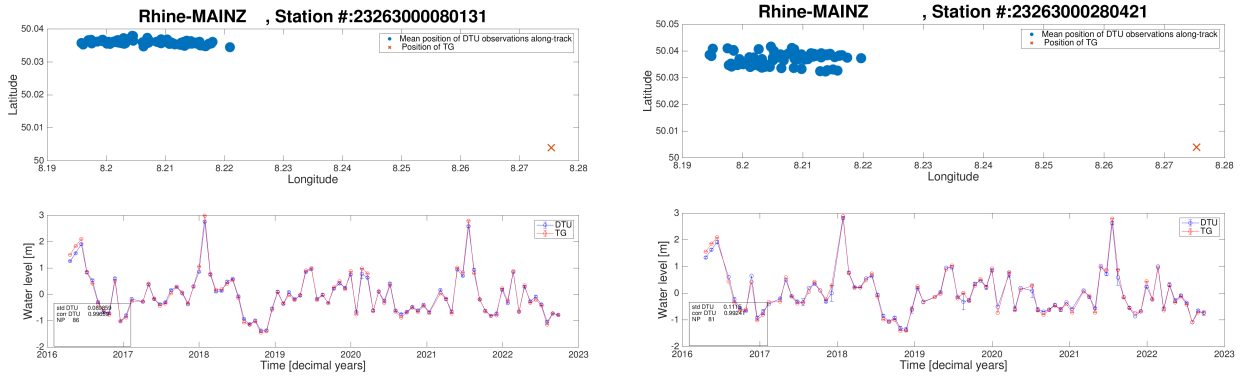


Figure 2.3 L3 and in-situ time-series in Mainz. L3 are from DTU (left) and from AHL (right).

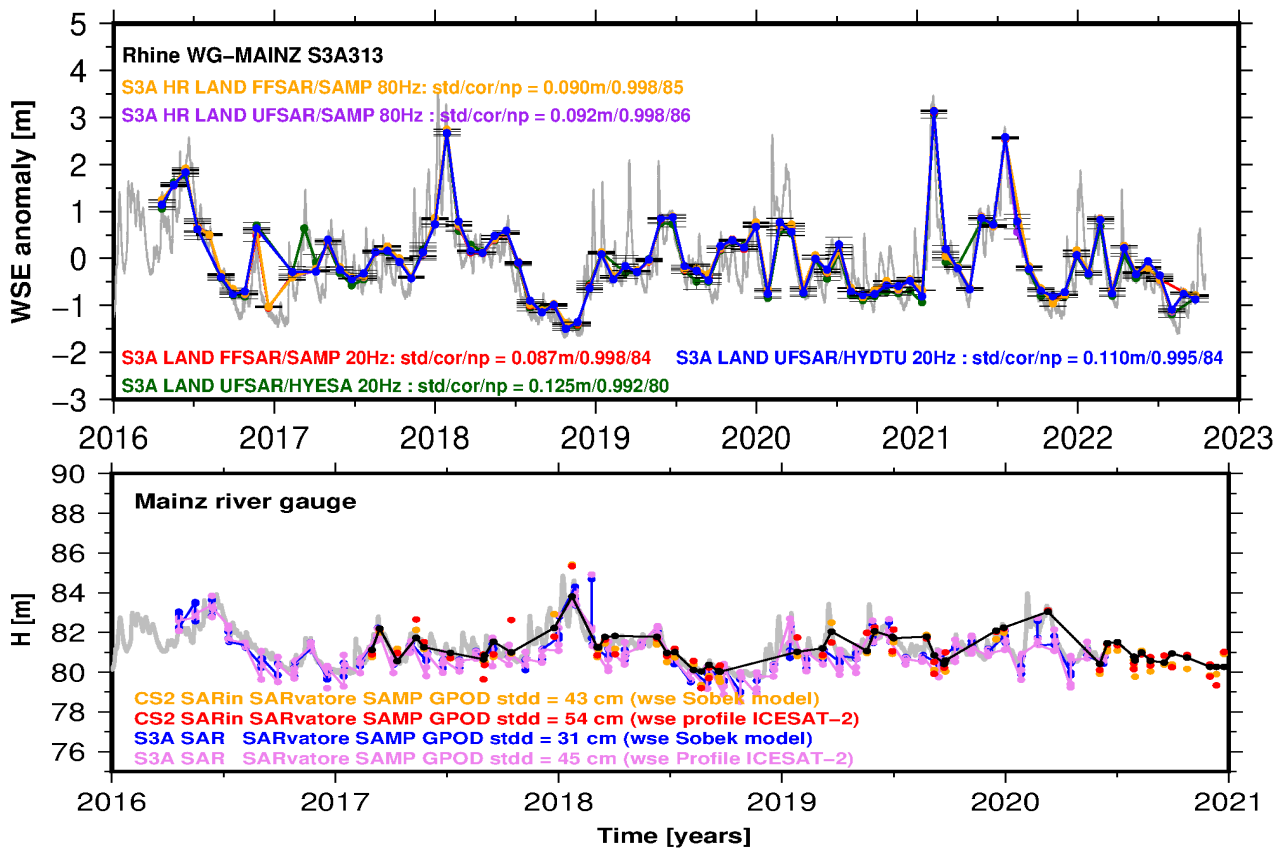


Figure 2.4 Altimetric time-series in Mainz for Sentinel-3A UFSAR 20 Hz DTU (blue) and ESA (green), UFSAR SARvatore SAMOSA+ (violet) and FFSAR/SAMP 80 Hz (orange) (above) and for CryoSat-2

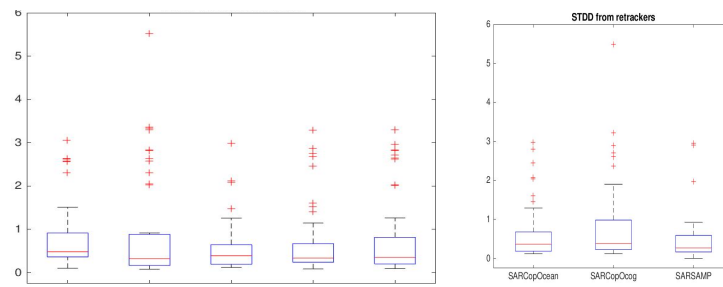


Figure 2.5 Boxplot of UFSAR products at the 42 VGs. Here all Hydrocoastal products and standard products are compared. The best accuracy is from SARvatore SAMP.

Table 2.4 River Rhine. Statistics at the eight VG in Figure 2.6

	20Hz-UFSAR DTU	20Hz-UFSAR ESA	20Hz-UFSAR-SAMP	80Hz- FFSAR-SAMP	80Hz- UFSAR-SAMP
Median	0.157	0.208	0.212	0.155	0.156
Mean	0.174	0.208	0.210	0.186	0.174

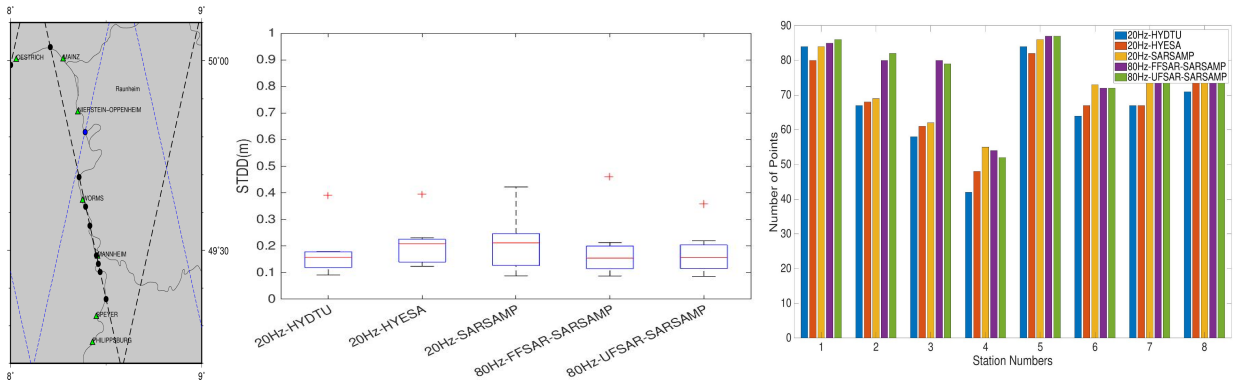


Figure 2.6 VGs Location S3A Track 313 (left), Boxplot of STDD (center) and number of points (right)

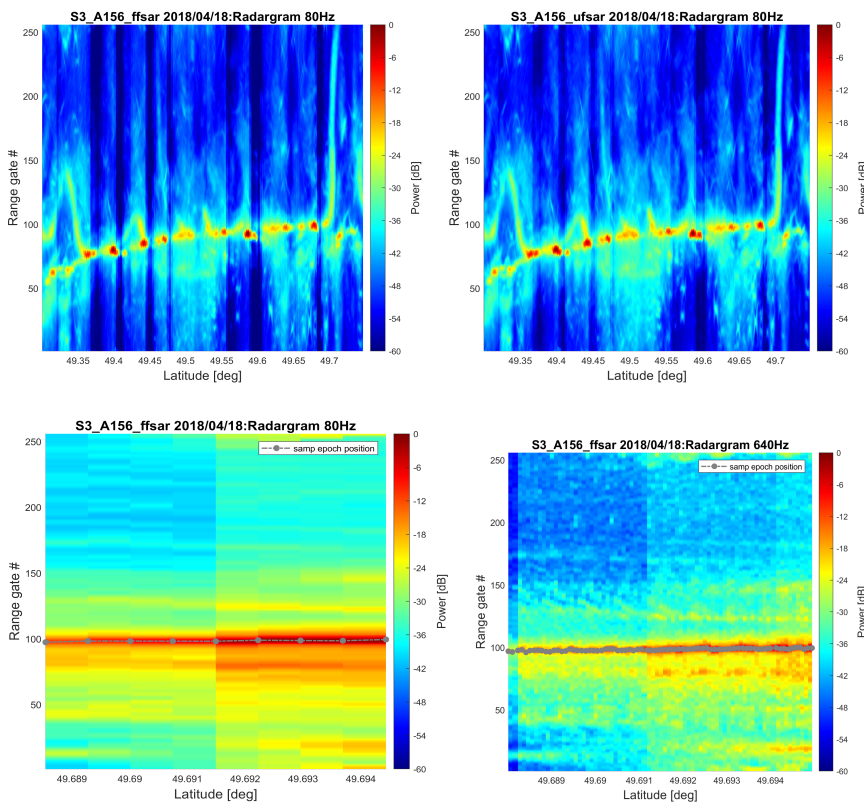


Figure 2.7 Comparison of radargrams in FFSAR and UFSAR at the 8 VGs locations (top) and of radargrams in FFSAR at 80 Hz and 640 Hz for Fig. 2.8 in Worms (bottom)

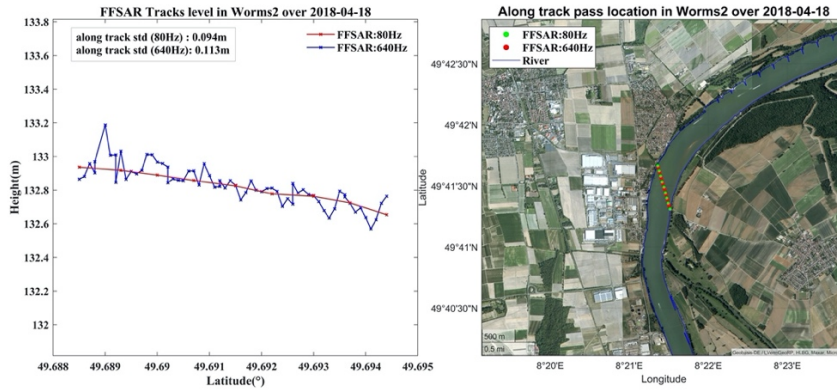


Figure 2.8 Along-track WSE in Worms at 80 and 640 Hz.

The river discharge is derived from space observations using the simple equation below that includes the Manning's roughness coefficient and the parameters water depth, river slope, river width. The observations are slope and the water level from altimetry and the discharge at in-situ stations. Width and depth of water are auxiliary parameters. Firstly channel conductance and the three exponents values suggested in Bjerklie (2005, Table 3) are used here (case 1). Secondly, we keep the exponents values fixed and estimate the conductance (case 2). Thirdly, the four parameters are derived in a least square adjustment. The slope is from altimetry and 15-min river discharge is from in-situ nearby stations. Case 3 gives the better results in terms of NS coefficient (0.93 in Worms, see Table 5). The third method is then applied to all the VGs where the slope can be used (Table 6) shows stable values for the estimated exponents and large change for the conductance k .

$$Q = k_2 W Y^{1.67} S^{0.33}$$

$$Y = f(H_{alti}) = H_{alti} - H_0$$

(Eq. 1-2-3)

$$S_{alti} = \frac{H_{altiWorms} - H_{altiMainz}}{L_{river}}$$

Table 2.5 River Rhine. Statistics in Worms using the three methods.

Model	N = 73	Log Residual	Relative Residual	Actual Residual	RMSE	MSC	NS	Qnorm	icase
Q=8.67 W ¹ Y ^{1.39} S ^{0.33}	mean	0.01	0.01	10.44	181.25	2.61	0.93	0.14	3
(adjusted coefficients)	std	0.12	0.12	182.22					
Q=23.3 W ¹ Y ^{1.67} S ^{0.5}	mean	-0.46	-0.36	-452.53	495.37	0.6	0.45	0.37	1
(Manning Equation)	std	0.15	0.11	202.93					
Q=7.14 W ¹ Y ^{1.67} S ^{0.33}	mean	-0.04	-0.03	-6.42	251.41	1.96	0.86	0.19	1
(Modified Manning equation)	std	0.14	0.14	253.09					
Q=25.2 W ¹ Y ^{1.5} S ^{0.5}	mean	-0.64	-0.47	-616.23	681.39	-0.04	-0.04	0.51	1
(Chezy equation)	std	0.13	0.07	292.82					
Q=7.73 W ¹ Y ^{1.5} S ^{0.33}	mean	-0.22	-0.19	-250.46	308.9	1.55	0.79	0.23	1
(Modified Chezy equation)	std	0.12	0.1	182.06					
Q=23.3 W ^{1.10} Y ^{1.67} S ^{0.5}	mean	0.07	0.09	154.34	359.09	1.25	0.71	0.27	1
(Regression Equation)	std	0.14	0.16	326.5					
Q=33.64 W ¹ Y ^{1.67} S ^{0.5}	mean	-0.09	-0.08	-58.98	266.33	1.84	0.84	0.2	2
(Adjusted Manning Equation)	std	0.15	0.15	261.54					
Q=6.94 W ¹ Y ^{1.67} S ^{0.33}	mean	-0.07	-0.06	-43.73	239.63	2.05	0.87	0.18	2
(Adjusted Modified Manning equation)	std	0.14	0.14	237.26					
Q=45.83 W ¹ Y ^{1.5} S ^{0.5}	mean	-0.04	-0.03	-24.62	224.21	2.18	0.89	0.17	2
(Adjusted Chezy equation)	std	0.13	0.14	224.42					
Q=9.43 W ¹ Y ^{1.5} S ^{0.33}	mean	-0.02	-0.02	-10.81	200.38	2.41	0.91	0.15	2
(Adjusted Modified Chezy equation)	std	0.12	0.12	201.49					
Q=4.21 W ^{1.10} Y ^{1.63} S ^{0.33}	mean	-0.07	-0.06	-39.44	237.4	2.07	0.87	0.18	2
(Adjusted Regression Equation)	std	0.14	0.14	235.74					

Table 2.6. River Rhine. Statistics for method number 3 (adjustment of the four parameters) at VGs where slope can be computed.

Station	NS	Qnorm	Exp. Width	Exp. depth	Exp. slope	K
Mainz	0.90	0.16	0.9	1.3	0.54	107.6
Worms	0.92	0.13	1.0	1.4	0.3	8.7
Duisburg	0.91	0.18	0.9	1.3	0.3	13.8
Wesel	0.93	0.15	0.9	1.3	0.3	3.7
Düsseldorf	0.86	0.22	0.9	1.3	0.3	14.9
Duisburg	0.94	0.15	0.9	1.3	0.68	335.8

The use an hydrological model using as input data Precipitation and evapo-transpiration. The monthly input data cover are Precipitation from IMERGE 2000.06-2021.09 and evapo-transpiration from GLEAM 1980-2022. We select as calibration interval the last 10 years (2010-2020), computation interval is 2000-2021. The NS in Table 7 is lower than 0.3 and the amplitude of the extremes is much lower in the model than in the input data (Fig. 2.10) We conclude that the simple monthly hydrological model is not best suited for our study and we will have to select a model with daily input data.

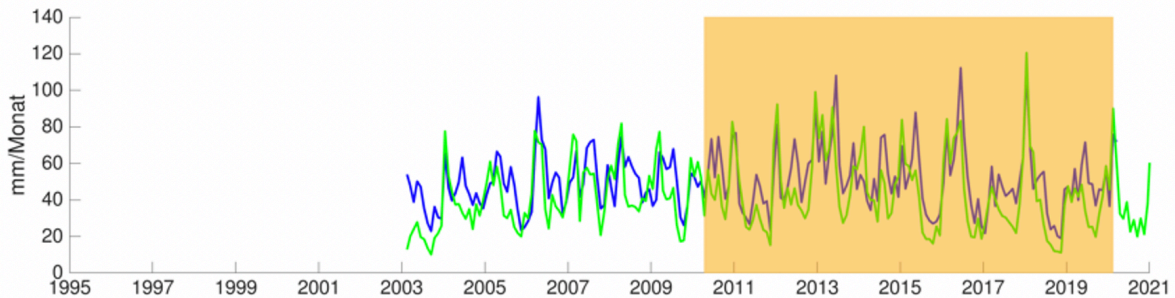
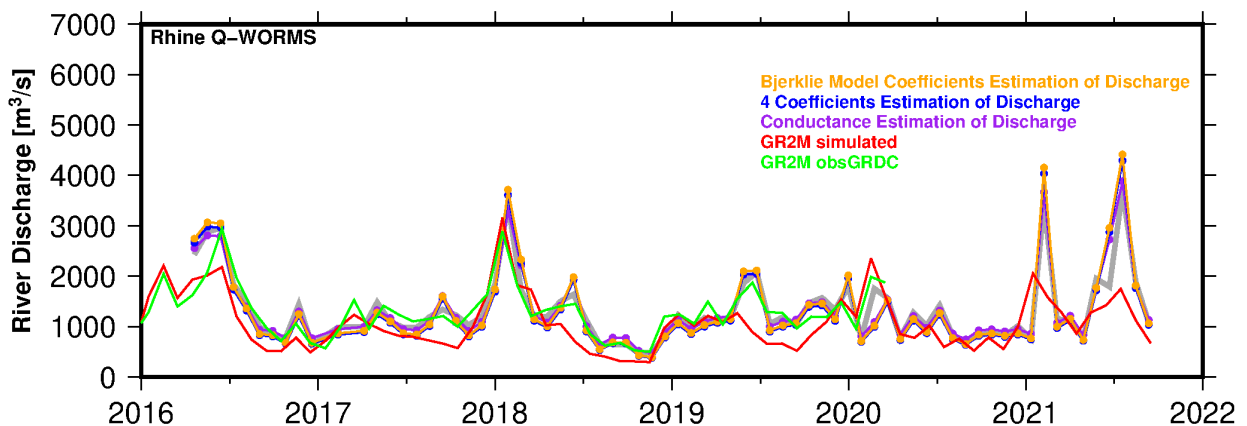


Figure 2.9 River discharge from simple hydrological model based on precipitation and evapo-transpiration.

Table 2.7 River Rhine. Hydrological model

Station	NS	Corr	RMSE (mm/mo)	QdM (bias)
Maxau	-0.1539	0.6583	21.692	0.786
Worms	0.1297	0.7317	15.476	0.855
Mainz	0.2513	0.7712	11.974	0.907
Kaub	0.2994	0.7850	11.248	0.916



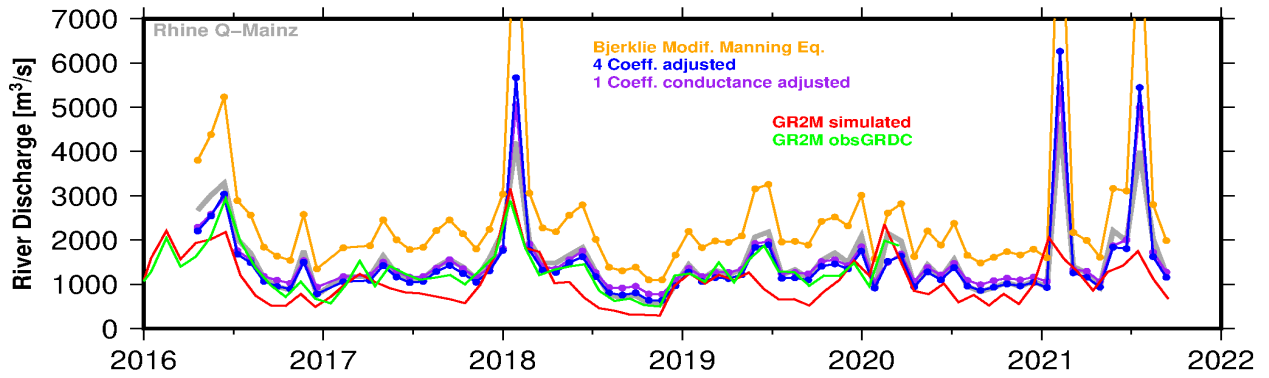


Figure 2.10 River discharge derived in Worms and in Mainz from the three approaches and from the GR2M model

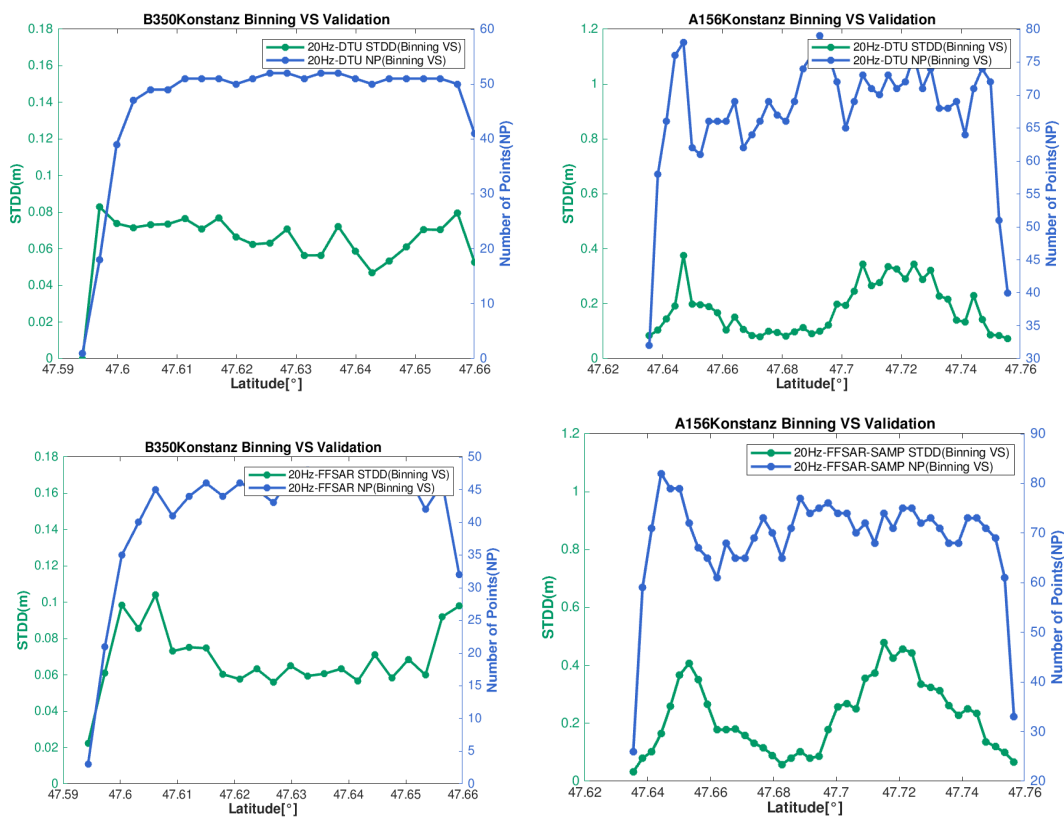


Figure 2.11 Accuracy of Water height in Lake of Constance from the DTU products (top) and from FFSAR (bottom). See location of ground tracks in Fig. 1.1 (right)

2.4 Summary

State of the art products have demonstrated that it is possible to enhance the quality and quantity of the altimeter data in rivers. The agreement with in-situ data depends on the method used for the comparison.

Moreover, for comparisons of along track data to nearby tide gauge the STDD, that measure of the accuracy, depend strongly on the region investigated and to its geophysical characteristics. The orientation of tracks is relevant.

Typical values for accuracy (STDD) found in literature are in the range 10-50 cm. With the HydroCoastal product, this study finds median values of 30 cm in the river Rhine. There is a clear consistency between the standard and the Hydrocoastal products. In UFSAR the best results are found using the Samosa+ retracker.

We have used the Fully Focused processing. This gives better spatial resolution along-track, results are good comparable to Samosa+ Earth Console as the same retracker is used, the accuracy is only slightly improved.

2.5 Highlight main findings

The case-study in inland water rivers and lakes shows that altimeter data exploitation is possible very near to coast. Contamination by land can however not be eliminated neither in USAR or in FF-SAR. In rivers the accuracy compared to the tide gauge is high (up to 10 cm). In lakes the accuracy can reach 6 cm, but varies along-track due to other effects, could be wind, to be investigated.

Some interesting findings that we mention hereinafter.

- Radargrams can be used to identify waveforms to be discarded
- Binned method is the preferable in the construction of the time-series
- Use of 80 hz instead than 20 hz is preferable in rivers

2.6 Potential Scientific / Operational Impact (“Benefit and unique value”)

Satellite altimetry in such an environment gives continuity of observations from open ocean through the coast and inland.

Comparison of results over different rivers width will bring better understanding on the limits of the technique.

2.7 Recommendations

The in depth altimeter data analyses outlined a number of topics to be addressed, including specific R&D investigations that deserve further consideration, with future projects to be implemented.

Hereinafter some recommendations:

- - Refine estimation of river slope variability from altimetry
 - Examine building a time-series (L3 data) and differences in WSE
 - Use for discharge estimation more complex hydrological models using daily inputs
 - Use for discharge estimation hydrodynamical models and coefficients variable in time
 - Investigate discharge at extremes
 - Investigate from multi-mission altimetry (2D altimetry and nadir together), SSH, slope and width, bathymetry with geophysical parameters variable in time
 - investigate FFSAR capability, consider difference of FFSAR results in sea and river, bays, lakes, contamination in all cases
 - Investigate SWOT early results of campaigns, River and Alpine lakes and reservoirs are an excellent cal/val test area for the 1-day SWOT, and all Sentinel-3,6 missions; climate change effect at high resolution are to be monitored from space
 - Consider methods (Bayesian) for tidal discharge and effect of wind, currents in the study

3. Acknowledgments

The authors want to thank the European Space Agency, which promoted and financed the HydroCoastal project

4. References

- Buchhaupt, C., Fenoglio-Marc, L., Becker, M., Kusche, J. (2021). Impact of Vertical Water Particle Motions on Fully-Focused SAR Altimetry. *Adv. Space Res.*, 68(2), pp. 853–874, doi.org/10.1016/j.asr.2020.07.015.
- Buchhaupt, C., Egido, A., Smith, W., Fenoglio, L. (2022). Conditional Sea Surface Statistics and Their Impact on Geophysical Sea Surface Parameters Retrieved From SAR Altimetry Signals, *Adv. Space Research*, <https://doi.org/10.1016/j.asr.2022.12.034>
- Bruni S., Fenoglio, L., Raicich, F., Zerbini, S. (2022). On the consistency of coastal sea level measurements in the Mediterranean Sea from tide gauge and satellite altimetry. *J. of Geodesy*, <https://doi.org/10.1007/s00190-022-01626-9>.
- Chen J., L. Fenoglio, K. Kusche, K. Liao, H. Uyanik, Z.A. Nazdir, Y. Lou (2023). Evaluation of Sentinel-3A altimetry over Songhua river basin, *J. of Hydrology*, <https://doi.org/10.1016/j.jhydrol.2023.129197>
- Dinardo, S., Fenoglio, L., Becker, M., Scharroo, R., Fernandes, M. J., Staneva, J., Grayek, S., Benveniste, J., (2020) A RIP-based SAR Retracker and its application in North East Atlantic with Sentinel-3, *Advances in Space Research*, Special Issue 25 Years of Satellite Altimetry, doi.org/10.1016/j.asr.2020.06.004.
- Dinardo, S., Restano, M., Ambrózio, A. and Benveniste, J., 2016, March. SAR altimetry processing on demand service for CryoSat-2 and Sentinel-3 at ESA G-POD. In *Proceedings of the 2016 conference on Big Data from Space (BiDS'16)*, Santa Cruz de Tenerife, Spain (pp. 15-17).
- Durand M. et al. included L. Fenoglio (2023). A framework for estimating global river discharge from the SWOT satellite mission, *Water Resources Research*, <https://doi.org/10.1029/2021WR031614>
- Fenoglio-Marc, L., S. Dinardo, R. Scharroo, A. Roland, M. Dutour Sikiric, B. Lucas, M. Becker, J. Benveniste, R. Weiss, 2015. The German Bight: A validation of CryoSat-2 altimeter data in SAR mode, *Advances in Space Research*, Volume 55, Issue 11, 2641-2656, ISSN 0273-1177, doi:10.1016/j.asr.2015.02.014.
- Fenoglio, L., Dinardo, S., Uebbing, B., Buchhaupt, C., Gärtner, M., Staneva, J., Becker, M., Klos, A., Kusche, J. (2021). Advances in NE-Atlantic coastal Sea Level Change Monitoring from Delay Doppler Altimetry, *Adv. Space Res.*,68(2), pp. 571–592, doi.org/10.1016/j.asr.2020.10.041.
- Fenoglio-Marc L., Buchhaupt C. (2020). TUDaBo a SAR Processing Prototype for GPOD, Altimetry coastal and Open Ocean Performance. Algorithm Theoretical Basis Doc., ESA, EOEP-SEOM-EOPS-TN-17-046
- Hossain, F., Bonnema, M. Srinivasan, M., Beighley, E., Andral, A. Doorn, B., Jayaluxmi, I., Jayasinghe, S., Kaheil, Y., Fatima, B., Elmer, N., Fenoglio, L., Bales, J., Lefevre, F., Legrand, S., Brunel, D., and Le Traon, P.Y. (2020). The Early Adopter Program for the Surface Water Ocean Topography Satellite Mission: Lessons Learned in Building User Engagement during the Pre-launch Era. *Bull. Amer. Meteor. Soc.* N. 101, doi.org/10.1175/BAMS-D-19-0235.1.
- Klos, A., Kusche, J., Fenoglio-Marc, L., Bos, M., Bogusz, J. (2019) Introducing a vertical land motion model for improving estimates of sea level rates derived from tide gauge records affected by earthquakes. *GPS Solut.*, 23: 102. doi.org/10.1007/s10291-019-0896-1
- International Altimetry Team (2021). Altimetry for the future: Building on 25 years of progress, *Adv. Space Res.*,68, pp. 319–363, <https://doi.org/10.1016/j.asr.2021.01.02>.
- Salameh, E., Frappart, F., Marieu, V., Spodar, A., Parisot, J.P., Hanquiez, V., Turki, I. and Laignel, B., 2018. Monitoring sea level and topography of coastal lagoons using satellite radar altimetry
- Schroeder, S., Springer, A., Kusche, A., Uebbing, B., Fenoglio, L., Diekkruieger, B., Pomeon, T. (2019). Niger discharge from radar altimetry: bridging gaps between gauge and altimetry time series *Hydrol. Earth Syst. Sci.*, 23, 4113–4128, 2019 <https://doi.org/10.5194/hess-23-4113-2019>